

Clusters, Radicals, and Ions; Environmental Chemistry

Fast Peroxy Radical Isomerization and OH Recycling in the Reaction of OH Radicals with Dimethyl Sulfide

Torsten Berndt, Wiebke Scholz, Bernhard Mentler, Lukas Fischer, Erik H. Hoffmann,
Andreas Tilgner, Noora Hyttinen, Nonne L. Prisle, Armin Hansel, and Hartmut Herrmann

J. Phys. Chem. Lett., **Just Accepted Manuscript** • DOI: 10.1021/acs.jpcllett.9b02567 • Publication Date (Web): 07 Oct 2019

Downloaded from pubs.acs.org on October 8, 2019

Just Accepted

"Just Accepted" manuscripts have been peer-reviewed and accepted for publication. They are posted online prior to technical editing, formatting for publication and author proofing. The American Chemical Society provides "Just Accepted" as a service to the research community to expedite the dissemination of scientific material as soon as possible after acceptance. "Just Accepted" manuscripts appear in full in PDF format accompanied by an HTML abstract. "Just Accepted" manuscripts have been fully peer reviewed, but should not be considered the official version of record. They are citable by the Digital Object Identifier (DOI®). "Just Accepted" is an optional service offered to authors. Therefore, the "Just Accepted" Web site may not include all articles that will be published in the journal. After a manuscript is technically edited and formatted, it will be removed from the "Just Accepted" Web site and published as an ASAP article. Note that technical editing may introduce minor changes to the manuscript text and/or graphics which could affect content, and all legal disclaimers and ethical guidelines that apply to the journal pertain. ACS cannot be held responsible for errors or consequences arising from the use of information contained in these "Just Accepted" manuscripts.

Fast Peroxy Radical Isomerization and OH Recycling in the Reaction of OH Radicals with Dimethyl Sulfide

T. Berndt,^{1*} W. Scholz,^{2,3} B. Mentler,² L. Fischer,² E. H. Hoffmann,¹ A. Tilgner,¹
N. Hyttinen,⁴ N. L. Prisle,⁴ A. Hansel,^{2,3} H. Herrmann¹

¹ Atmospheric Chemistry Dept. (ACD), Leibniz Institute for Tropospheric Research (TROPOS), 04318 Leipzig, Germany.

² Institute for Ion Physics and Applied Physics, University of Innsbruck, 6020 Innsbruck, Austria.

³ IONICON Analytik GmbH, 6020 Innsbruck, Austria.

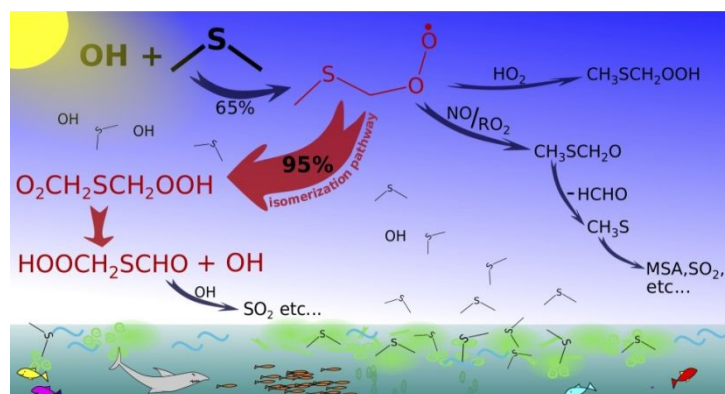
⁴ Nano and Molecular Systems Research Unit, University of Oulu, 90014 Oulu, Finland.

*Correspondence to: T. Berndt (berndt@tropos.de)

Abstract

Dimethyl sulfide (DMS), produced by marine organisms, represents the most abundant, biogenic sulfur emission into the Earth's atmosphere. The gas-phase degradation of DMS is mainly initiated by the reaction with the OH radical forming first $\text{CH}_3\text{SCH}_2\text{O}_2$ radicals from the dominant H-abstraction channel. It is experimentally shown that these peroxy radicals undergo a two-step isomerization process finally forming a product consistent with the formula HOCH_2SCHO . The isomerization process is accompanied by OH recycling. The rate-limiting first isomerization step, $\text{CH}_3\text{SCH}_2\text{O}_2 \rightarrow \text{CH}_2\text{SCH}_2\text{OOH}$, followed by O_2 addition, proceeds with $k = (0.23 \pm 0.12) \text{ s}^{-1}$ at $295 \pm 2 \text{ K}$. Competing bimolecular $\text{CH}_3\text{SCH}_2\text{O}_2$ reactions with NO, HO_2 or RO_2 radicals are less important for trace-gas conditions over the oceans. Results of atmospheric chemistry simulations demonstrate the predominance ($\geq 95\%$) of $\text{CH}_3\text{SCH}_2\text{O}_2$ isomerization. The rapid peroxy radical isomerization, not yet considered in models, substantially changes the understanding of DMS's degradation processes in the atmosphere.

TOC Graphic



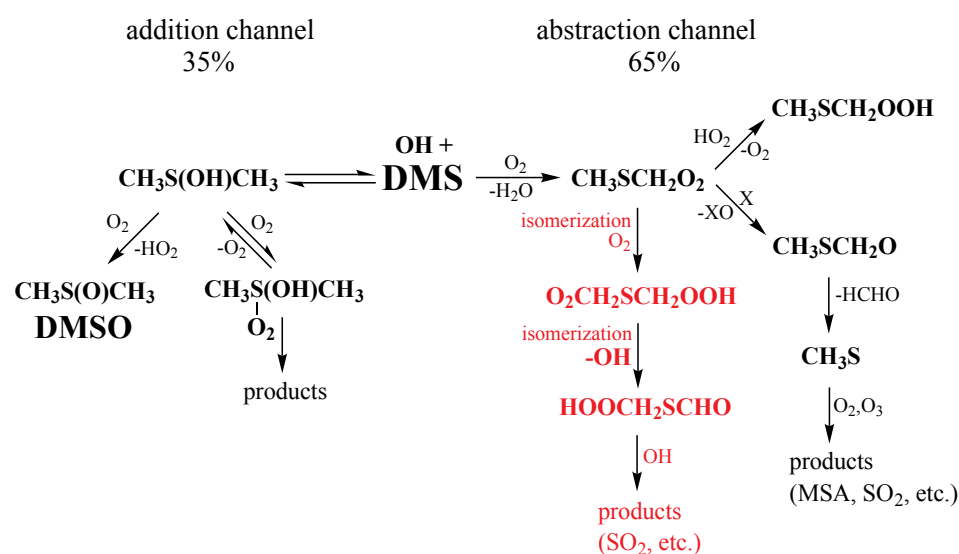
The emission of dimethyl sulfide (DMS: CH_3SCH_3) over the oceans is the largest natural sulfur source to the Earth's atmosphere with an estimated rate of $(10 - 35) \times 10^6$ metric tons of sulfur per year.¹⁻⁶ Gas-phase oxidation of DMS, mainly initiated by the reaction with OH radicals, leads to the formation of sulfuric acid (H_2SO_4) and methane sulfonic acid (MSA: $\text{CH}_3\text{SO}_3\text{H}$)⁷ which are important for the formation of natural aerosols and clouds in the marine boundary layer.^{8,9} Natural aerosols, including those from DMS oxidation, are assumed to account for the largest uncertainty of aerosol's radiative forcing in climate models.¹⁰

A series of kinetic studies in absence and presence of molecular oxygen consistently describe the occurrence of two independent channels of the OH + DMS reaction, i.e. i) the reversible OH addition forming the adduct radical $\text{CH}_3\text{S}(\text{OH})\text{CH}_3$ and ii) the H atom abstraction pathway forming the peroxy radical $\text{CH}_3\text{SCH}_2\text{O}_2$ after subsequent O_2 addition.^{7, 11-13} The addition / abstraction branching ratio of about 35 / 65 can be derived from kinetic measurements between 295 to 299 K at atmospheric O_2 concentration. The experimentally observed molar formation yield of dimethyl sulfoxide (DMSO: $\text{CH}_3\text{S}(\text{O})\text{CH}_3$) of $35 \pm 8\%$ at 295 K¹⁴ supports this branching ratio supposing DMSO as the predominate 1st generation product from the addition channel.⁷

The knowledge regarding the 1st generation product formation from the abstraction channel, however, is still sparse despite a large number of experimental and theoretical studies in the past.⁷ It is assumed up to now and implemented in current models¹⁵ that the primarily formed $\text{CH}_3\text{SCH}_2\text{O}_2$ radical reacts in the atmosphere with NO,¹⁶⁻¹⁸ HO_2 ¹⁹ and RO_2 radicals^{16,18}. The main product of the $\text{CH}_3\text{SCH}_2\text{O}_2 + \text{NO}$ reaction is the corresponding alkoxy radical, $\text{CH}_3\text{SCH}_2\text{O}$, which has been suggested to rapidly decompose forming HCHO and CH_3S .¹⁸ CH_3S is believed to be the key intermediate forming MSA as well as SO_2 , which leads to H_2SO_4 production from its OH radical reaction in the presence of water vapor.⁷ $\text{CH}_3\text{SCH}_2\text{OOH}$ formation is assumed from the $\text{CH}_3\text{SCH}_2\text{O}_2 + \text{HO}_2$ reaction analogous to the hydroperoxide channel known from a series of $\text{RO}_2 + \text{HO}_2$ reactions.^{7,19} The $\text{CH}_3\text{SCH}_2\text{O}_2 + \text{RO}_2$ reaction proceeds either via the reduction channel forming $\text{CH}_3\text{SCH}_2\text{O}$, that rapidly results in HCHO and CH_3S , or via the dismutation channel forming $\text{CH}_3\text{SCH}_2\text{OH}$ and CH_3SCHO .^{7,19} A HCHO formation yield of unity has been reported from the $\text{CH}_3\text{SCH}_2\text{O}_2$ self-reaction emphasizing the predominance of the reduction channel in this case.¹⁸

Results of a recent theoretical study, however, propose rapid isomerization of the $\text{CH}_3\text{SCH}_2\text{O}_2$ radical that could be able to outrun the rate of the bimolecular $\text{CH}_3\text{SCH}_2\text{O}_2$ reactions for typical NO, HO_2 and RO_2 radical concentrations present over the oceans.²⁰

Findings of the calculations indicate the occurrence of a new peroxy radical $\text{O}_2\text{CH}_2\text{SCH}_2\text{OOH}$ that is formed from $\text{CH}_3\text{SCH}_2\text{O}_2$ isomerization with subsequent O_2 addition. A next isomerization step can occur resulting in HOCH_2SCHO and an OH radical. It is to be noted, that an analog sequence of RO_2 radical isomerization steps has been reported from the low-temperature combustion of dimethyl ether forming the analog HOCH_2OCHO as a closed-shell product.²¹ Experimental evidence for these processes from the $\text{OH} + \text{DMS}$ reaction and kinetic measurements of the $\text{CH}_3\text{SCH}_2\text{O}_2$ isomerization do not exist up to now. Previous DMS product studies in the laboratory were affected by insufficient product detection sensitivity and by too high NO , HO_2 or RO_2 radical levels in the experiments, suppressing possible isomerization steps of peroxy radicals by excessive bimolecular reaction rates.^{14, 22-24} Scheme 1 summarizes the current knowledge on the first steps of the $\text{OH} + \text{DMS}$ reaction in the literature⁷ along with the proposed reaction scheme based on theoretical calculations.²⁰ The formation of SO_2 has been proposed from the subsequent $\text{OH} + \text{HOCH}_2\text{SCHO}$ reaction.²⁰



Scheme 1. First reaction steps of the $\text{OH} + \text{DMS}$ reaction, the established scheme from the review by Barnes *et al.*⁷ in black and proposed pathways from theoretical calculations²⁰ in red. Detected products from the present study are given in bold red. “X” stands for the reactants NO and RO_2 that can reduce the peroxy radical to the corresponding alkoxy radical.

Here we report on results of a mechanistic study of the $\text{OH} + \text{DMS}$ reaction with focus on the 1st generation products from the abstraction channel. Experiments have been conducted at 295 ± 2 K and 1 bar of purified air in a free-jet flow system, that allows for investigations in the absence of wall interactions for a reaction time of 7.9 s.^{25,26} The chosen reaction

conditions ensured monitoring of the possible $\text{CH}_3\text{SCH}_2\text{O}_2$ isomerization products without interference from bimolecular $\text{CH}_3\text{SCH}_2\text{O}_2$ reactions. Product formation was followed either by a chemical ionization - atmospheric pressure interface - time-of-flight mass spectrometer (CI-API-TOF) using iodide (I^-)^{27,28}, acetate (CH_3COO^-)^{29,30}, protonated n-propylamine ($\text{n-C}_3\text{H}_7\text{NH}_3^+$)³¹ or protonated acetone ($((\text{CH}_3)_2\text{CO-H}^+)$)³² as the reagent ion or by a chemical ionization - time-of-flight mass spectrometer (CI3-TOF) applying ammonium (NH_4^+)^{33,34} for product ionization at reduced pressure. Quantum chemical calculations support the assessment of used ionization schemes for product detection (see Supporting Information). OH radicals were formed from ozonolysis of tetramethylethylene (TME)³⁵ or, alternatively, via isopropyl nitrite photolysis.³⁶

Sensitive detection of the sulfur containing products has been achieved using I-CI-API-TOF analysis for a DMS conversion down to 4×10^6 molecules cm^{-3} . Observed signals in the mass spectra are consistent with the formation of the peroxy radical $\text{O}_2\text{CH}_2\text{SCH}_2\text{OOH}$ from $\text{CH}_3\text{SCH}_2\text{O}_2$ isomerization, pathway (1), as well as the closed-shell product $\text{HOOCH}_2\text{SCHO}$ from a subsequent isomerization step followed by rapid decomposition of the unstable $\text{HOOCH}_2\text{SCHOOH}$ ²⁰ via pathway (2) (see the black spectrum in Figure 1 and Figure S1 for conditions of isopropyl nitrite photolysis).



These products are in accordance with predictions from theoretical calculations.²⁰ An additional weak signal attributed to $\text{C}_2\text{H}_6\text{O}_4\text{S}$, possibly $\text{HOOCH}_2\text{SCH}_2\text{OOH}$ formed via $\text{RO}_2 + \text{HO}_2 \rightarrow \text{ROOH} + \text{O}_2$, became detectable for higher DMS conversions with higher HO_2 radical levels (see Figure S1). (HO_2 radicals are formed along with DMSO via the addition channel and from other pathways mainly related to the OH radical generation.) On the other hand, signals of $\text{CH}_3\text{SCH}_2\text{O}_2$ have not been detected with any of the ionization schemes applied. The $\text{CH}_3\text{SCH}_2\text{O}_2$ adducts with the used reagent ions are not stable enough for the successful detection as shown by quantum chemical calculations (see details in Supporting Information). DMSO, formed from the addition channel, was detectable by all ionization techniques, but will be not further discussed here.

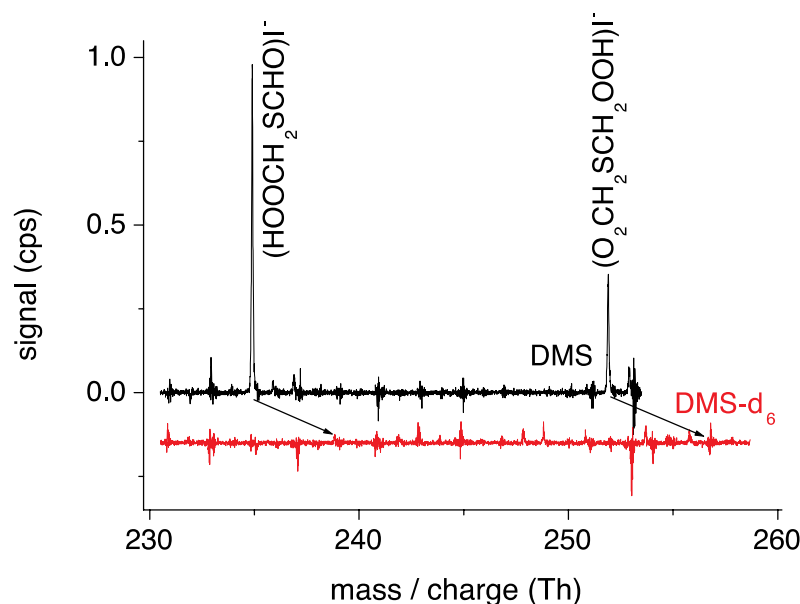


Figure 1. Background corrected spectra from OH + DMS (black spectrum) and OH + DMS- d_6 (red spectrum) using I-CI-APi-TOF analysis and TME ozonolysis for OH formation. The calculated DMS conversion is 4.5×10^7 molecules cm^{-3} and that of DMS- d_6 ³⁷ about 2.8×10^7 molecules cm^{-3} . Reactant concentrations are $[\text{O}_3] = 1.6 \times 10^{11}$, $[\text{TME}] = 3 \times 10^{10}$, $[\text{DMS}]$ or $[\text{DMS-}d_6] = 5 \times 10^{12}$ molecules cm^{-3} .

The corresponding product formation starting from OH + DMS- d_6 was also tested for otherwise identical reaction conditions (see red spectrum in Figure 1). While the $\text{CD}_3\text{SCD}_2\text{O}_2$ formation rate is already slowed down by a factor of 2.4 compared to the rate of the non-deuterated compound³⁷, intramolecular D-shifts in the course of peroxy radical isomerization are assumed to be much slower than the corresponding H-shifts in non-deuterated compounds. For instance, a deceleration factor of about 15 has been found for D-shifts in the isoprene system.³⁸ Hence, absence of the expected $\text{O}_2\text{CD}_2\text{SCD}_2\text{OOD}$ and $\text{DOOCD}_2\text{SCDO}$ signals clearly above background level is consistent with an isomerization mechanism (intramolecular H-shifts) leading to the observed products from the abstraction channel.

Addition of propane, acting as OH radical scavenger, led to total product suppression. This behavior demonstrates that the observed products exclusively arose from OH + DMS, not affected by any reactions of ozonolysis products with DMS under ozonolysis conditions (see Figure S2). The product concentrations increased linearly with rising DMS conversion in line with the first-order kinetics of product formation from radical isomerization via pathways (1) and (2) (see Figure 2). Based on results of reaction modeling in the flow system, bimolecular $\text{CH}_3\text{SCH}_2\text{O}_2$ reactions consumed less than 0.2% of the formed $\text{CH}_3\text{SCH}_2\text{O}_2$ radicals for DMS

conversions $< 5 \times 10^7$ molecules cm^{-3} ensuring fully undisturbed reaction conditions for radical isomerization steps.

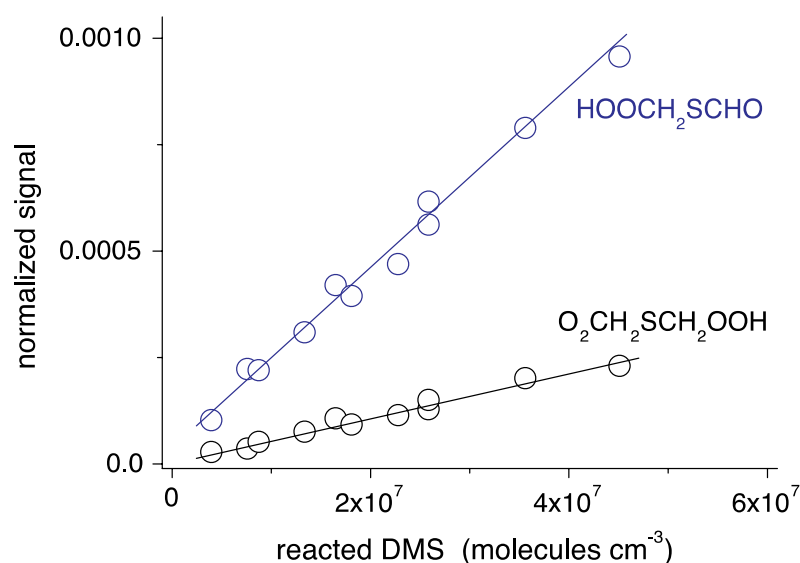


Figure 2. Product formation from OH + DMS as a function of calculated DMS conversion. Analysis was carried out by I-CI-APi-TOF and TME ozonolysis served as the OH radical source. Reactant concentrations are $[\text{O}_3] = (2.7 - 16) \times 10^{10}$, $[\text{TME}] = 1.5$ or 3.0×10^{10} and $[\text{DMS}] = 2.5$ or 5.0×10^{12} molecules cm^{-3} .

Product analysis for elevated DMS conversion applying other ionization techniques confirmed the findings as observed by I⁻ ionization. Both isomerization products, as well as $\text{C}_2\text{H}_6\text{O}_4\text{S}$, have been measured by means of NH_4^+ -CI3-TOF (see Figure S3). There was no indication for the occurrence of further products from the abstraction channel. Generally, the lack of justified calibration factors prevents the determination of absolute product concentrations. However, results obtained by NH_4^+ -CI3-TOF and I-CI-APi-TOF consistently point to $\text{HOOCH}_2\text{SCHO}$ as the predominant reaction product based on its signal strength compared with that of $\text{O}_2\text{CH}_2\text{SCH}_2\text{OOH}$. The formation of $\text{HOOCH}_2\text{SCHO}$ was also detected by CH_3COO^- - and $(\text{CH}_3)_2\text{CO-H}^+$ -CI-APi-TOF (see Figures S4 and S5).

The kinetics of the $\text{CH}_3\text{SCH}_2\text{O}_2$ isomerization relative to the $\text{CH}_3\text{SCH}_2\text{O}_2 + \text{NO}$ reaction, i.e. the ratio of the rate coefficients k_1 / k_3 , has been obtained by monitoring the $\text{CH}_3\text{SCH}_2\text{O}_2$ isomerization products for rising NO concentrations. (The individual rate coefficients belong to the reaction pathways with the same numbering.)



At the same time, addition of NO to the reaction gas led to increasing OH radical formation via the $\text{NO} + \text{HO}_2 \rightarrow \text{OH} + \text{NO}_2$ reaction, and consequently enhanced product formation from $\text{OH} + \text{DMS}$ (see Figure 3A). Lowering of the HO_2 radical concentration with rising NO became clearly visible following the $(\text{HO}_2)\text{I}^-$ signal³⁹ (see Figure 3A). Increasing OH levels were indirectly monitored by the SO_3 formation via the reaction sequence $\text{OH} + \text{SO}_2 \rightarrow \text{HOSO}_2$ and $\text{HOSO}_2 + \text{O}_2 \rightarrow \text{SO}_3 + \text{HO}_2$.⁴⁰ SO_2 additives were chosen in such a way that $\text{OH} + \text{SO}_2$ did not disturb the $\text{OH} + \text{DMS}$ reaction, i.e. a reaction rate ratio $r(\text{OH}+\text{SO}_2) / r(\text{OH}+\text{DMS}) = 0.05$. The measured SO_3 signal, standing for the integral OH radical concentration, enables the normalization of the isomerization product formation for changing OH radical conditions (see Figure 3B). The normalized signals of $\text{O}_2\text{CH}_2\text{SCH}_2\text{OOH}$ and $\text{HOOCH}_2\text{SCHO}$ declined parallel to each other with rising NO consistent with the behavior of isomerization products from the consecutive reaction pathways (1) and (2). The second isomerization step is supposed to be much faster than the first one based on theoretical calculations stating $k_1 = 2.1 \text{ s}^{-1}$ and $k_2 = 73 \text{ s}^{-1}$ at 293 K.²⁰ That means that pathway (1) is rate limiting for the $\text{CH}_3\text{SCH}_2\text{O}_2$ isomerization process. The rapid $\text{O}_2\text{CH}_2\text{SCH}_2\text{OOH}$ isomerization via pathway (2) represses the importance of its bimolecular reaction with NO. Hence, the $\text{O}_2\text{CH}_2\text{SCH}_2\text{OOH} + \text{NO}$ reaction has been neglected in the data analysis. The normalized signals of the $\text{CH}_3\text{SCH}_2\text{O}_2$ isomerization products as a function of NO at a fixed reaction time t , $[\text{iso-prod}]_t^{\text{norm}} = f([\text{NO}])$, allow the determination of $B = k_1 / k_3$ from Eq.(I) (see Supporting Information).

$$[\text{iso-prod}]_t^{\text{norm}} = A / (1 + [\text{NO}]/B) \quad (\text{I})$$

The analysis yielded $k_1 / k_3 = (2.1 \pm 0.4) \times 10^{10}$ and $(1.5 \pm 0.3) \times 10^{10} \text{ molecule cm}^{-3}$ for the decline of $\text{HOOCH}_2\text{SCHO}$ and $\text{O}_2\text{CH}_2\text{SCH}_2\text{OOH}$ (Figure 3B), respectively, leading to the mean value $k_1 = 0.23 \pm 0.12 \text{ s}^{-1}$ based on $k_3 = (1.3 \pm 0.6) \times 10^{-11} \text{ cm}^3 \text{ molecule}^{-1} \text{ s}^{-1}$ taken from the literature data¹⁶⁻¹⁸.

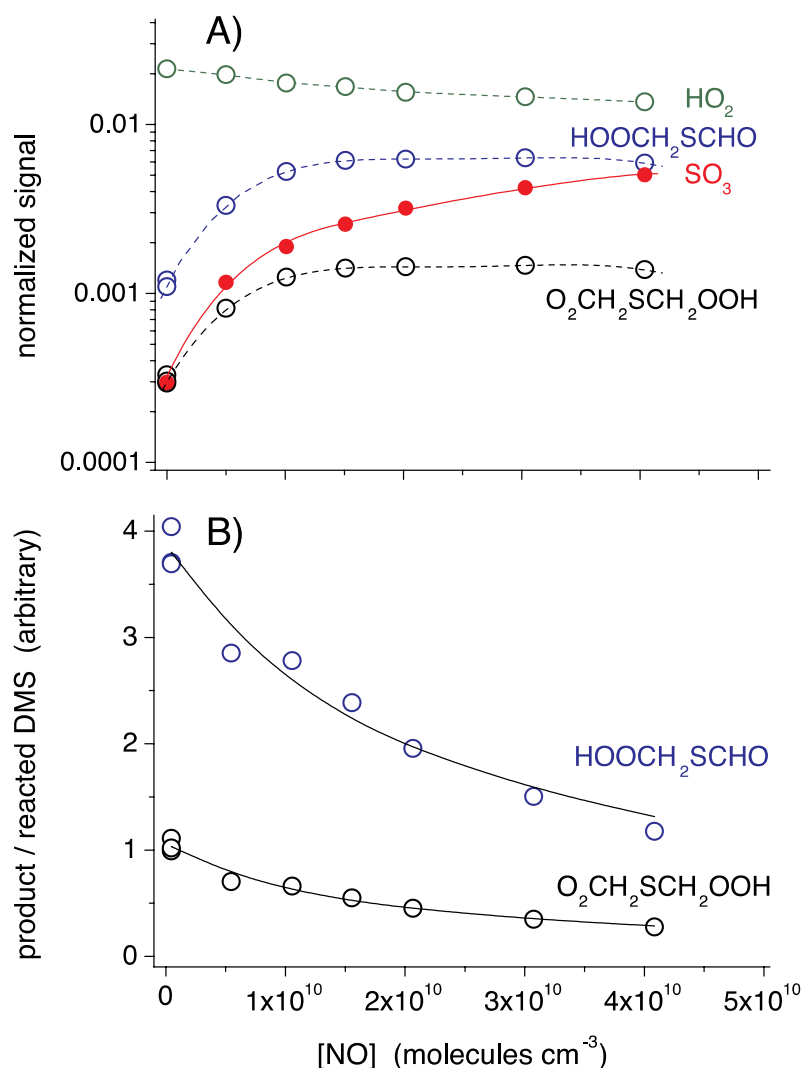


Figure 3. Product formation from OH + DMS as a function of NO using OH radical formation via isopropyl nitrite photolysis. **A** Concentrations of isomerization products and HO₂ radicals measured by I-CI-APi-TOF and SO₃ formation by n-C₃H₇NH₃⁺-CI-APi-TOF. **B** Normalized isomerization product signals considering changing DMS conversion with rising NO due to enhanced OH radical production. The lines show the best fit results from kinetic analysis of k_1 / k_3 . Reactant concentrations are [isopropyl nitrite] = 5.0×10^{10} , [SO₂] = 1.5×10^{12} , [DMS] = 5.0×10^{12} and [NO] = $(5.0\text{--}40.4) \times 10^9$ molecules cm⁻³. The final NO concentration from isopropyl nitrite photolysis has been calculated to be 9.3×10^8 molecules cm⁻³.

Furthermore, the OH recycling has been probed, which is expected as an associated product channel of the HOOCH₂SCHO formation via pathway (2). SO₃ formation from OH + SO₂, as a measure of the integral OH radical concentration, has been followed for conditions of a fixed OH formation rate via isopropyl nitrite photolysis and a constant OH consumption rate via OH + hydrocarbon (HC) or OH + DMS, i.e. $k(\text{OH}+\text{HC}) \times [\text{HC}] = k(\text{OH}+\text{DMS}) \times [\text{DMS}] = \text{constant}$. The selected HCs were TME, α -pinene and decalin. The needed rate coefficients $k(\text{OH}+\text{HC})$ at room temperature are available with good precision in

the literature, i.e. $k(\text{OH}+\text{TME}) = 1.1 \times 10^{-10} \text{ s}^{-1}$, $k(\text{OH}+\alpha\text{-pinene}) = 5.33 \times 10^{-11} \text{ s}^{-1}$ and $k(\text{OH}+\text{cis/trans-decalin}) = 2.03 \times 10^{-11} \text{ cm}^3 \text{ molecule}^{-1} \text{ s}^{-1}$. The latter represents the mean value of the individual rate coefficients of both isomers.⁴² The SO_2 additive also consumed a constant, minor fraction of OH, again with the reaction rate ratio $r(\text{OH}+\text{SO}_2) / r(\text{OH}+\text{HC}(\text{or DMS})) = 0.05$ in order to keep the OH + HC(or DMS) reaction less influenced. If no OH recycling occurs, constant OH formation and loss terms result in a constant integral OH radical concentration (constant SO_3 signal) independent of the HC(or DMS) used. This behavior was visible in the case of TME, α -pinene and decalin where OH recycling has not been reported so far in the literature (see Figure 4). For OH + DMS, however, the SO_3 signal increased by about 55% relative to the other reaction systems indicating efficient OH recycling. Model calculations show an increase of the integral OH radical concentration by 43% due to $\text{CH}_3\text{SCH}_2\text{O}_2$ isomerization with $k_1 = 0.23 \text{ s}^{-1}$ for the reaction time of 7.9 s in the experiment. This measurement supports the rapid $\text{CH}_3\text{SCH}_2\text{O}_2$ isomerization including OH recycling being at least as fast as determined from the competition kinetics as shown before.

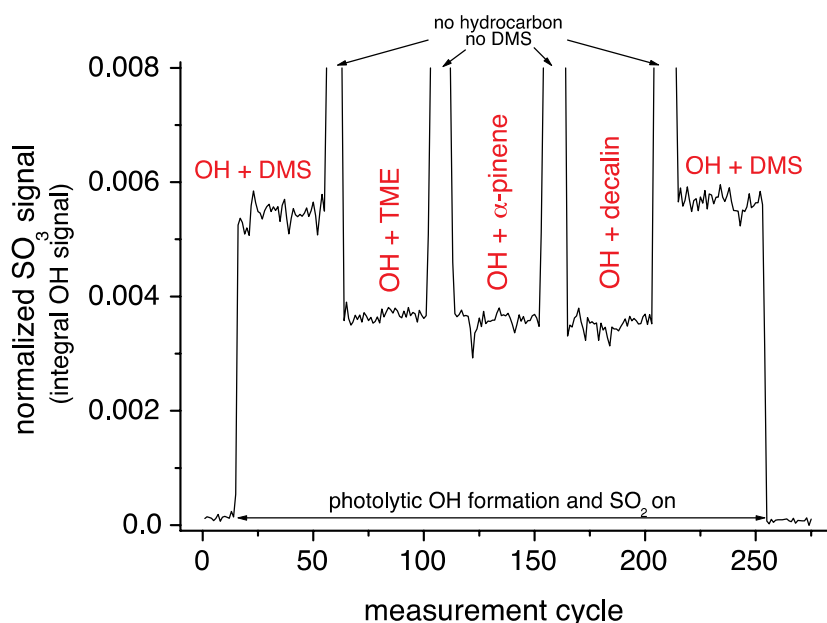


Figure 4. SO_3 signal, standing for the integral OH radical concentration, measured for constant OH production via isopropyl nitrite photolysis and constant OH consumption via OH + hydrocarbon (HC) or OH + DMS, HCs: TME, α -pinene and decalin. No SO_3 signal has been measured in the absence of the SO_2 additive. One measurement cycle comprises 60 s data accumulation. Reactant concentrations are $[\text{isopropyl nitrite}] = 4.5 \times 10^{11}$, $[\text{SO}_2] = 5.01 \times 10^{11}$, $[\text{DMS}] = 1.67 \times 10^{12}$, $[\text{TME}] = 1.18 \times 10^{11}$, $[\alpha\text{-pinene}] = 2.44 \times 10^{11}$ and $[\text{cis/trans-decalin}] = 6.40 \times 10^{11} \text{ molecules cm}^{-3}$.

Multiphase chemistry investigations with an air parcel model were carried out to validate the impact of the $\text{CH}_3\text{SCH}_2\text{O}_2$ isomerization process for pristine ocean conditions at 295 K (see Figure S6).^{43,44} The model results clearly demonstrate that isomerization dominates the chemical fate of $\text{CH}_3\text{SCH}_2\text{O}_2$. The mean contribution ranges from 95 to 98.5% considering $k_1 = 0.23 \pm 0.12 \text{ s}^{-1}$ within its range of uncertainty (see Figure S7). Average concentrations of NO, HO_2 and total RO_2 radicals in the model were 6×10^6 , 1×10^8 and $4 \times 10^8 \text{ molecules cm}^{-3}$ resulting in pseudo first-order rate coefficients of the corresponding bimolecular $\text{CH}_3\text{SCH}_2\text{O}_2$ reactions of 7.0×10^{-5} , 1.0×10^{-3} and $1.5 \times 10^{-3} \text{ s}^{-1}$ at 295 K, respectively. The dominance of the isomerization process entails consequences for the OH budget and the subsequent product formation. The simulations reveal that the isomerization process increases the total OH radical formation rate by 2% on average and by 17% during nighttime when $\text{CH}_3\text{SCH}_2\text{O}_2$ formation via $\text{NO}_3 + \text{DMS}$ ^{7,45} is active (see Figure S8). Furthermore, MSA formation from consecutive reactions of $\text{HOOCH}_2\text{SCHO}$ is impossible because no methyl group is left in this molecule. Hence, MSA formation from the abstraction channel, as thought up to now via the CH_3S intermediate^{7,15}, is inhibited leading to reduction of the modeled gas-phase MSA concentration by 30% (see Figure S9). HOOCH_2S formation from the subsequent $\text{OH} + \text{HOOCH}_2\text{SCHO}$ reaction via H abstraction and CO elimination has been proposed, that finally leads to SO_2 and HCHO including OH recycling.²⁰ This scenario, however, is speculative at the moment and needs experimental verification. Moreover, $\text{HOOCH}_2\text{SCHO}$ could be also subject to the particle-phase chemistry because of its high oxidation state and the expected partitioning into the particle phase.

In conclusion, 1st generation product formation from the abstraction channel of the $\text{OH} + \text{DMS}$ reaction has been investigated at $295 \pm 2 \text{ K}$ and atmospheric pressure of air. The experimental findings reveal a two-step isomerization process of $\text{CH}_3\text{SCH}_2\text{O}_2$ radicals finally forming $\text{HOOCH}_2\text{SCHO}$ accompanied by OH recycling. This process is in accordance with predictions based on theoretical calculations.²⁰ The rate-limiting first isomerization step, $\text{CH}_3\text{SCH}_2\text{O}_2 \rightarrow \text{CH}_2\text{SCH}_2\text{OOH}$, proceeds with $k = (0.23 \pm 0.12) \text{ s}^{-1}$ at $295 \pm 2 \text{ K}$. This rate coefficient is about one order of magnitude smaller than the result of the theoretical calculations²⁰. The $\text{CH}_3\text{SCH}_2\text{O}_2$ isomerization process is clearly faster than the traditional bimolecular $\text{CH}_3\text{SCH}_2\text{O}_2$ reactions with NO, HO_2 and RO_2 radicals for trace gas conditions over the oceans accounting for $\geq 95\%$ of the $\text{CH}_3\text{SCH}_2\text{O}_2$ removal as shown by a modeling study at 295 K. Continuing experimental work is needed in order to discover the 2nd generation product formation with special attention to SO_2 and MSA.

Acknowledgements

The authors thank K. Pielok and A. Rohmer for technical assistance and the tofTools team for providing the data analysis tools. NH thanks CSC - IT Center for Science, Finland, for computational resources. The project was partly funded by the European Research Council (ERC) under the European Union's Horizon 2020 research and innovation program, Project SURFACE (Grant Agreement No. 717022). NH and NLP also gratefully acknowledge the financial contribution from the Academy of Finland (Grant Nos. 308238 and 314175). WS received funding from the European Union's Horizon 2020 research and innovation program (Marie Skłodowska-Curie grant agreement No. 764991).

Note

The authors declare no competing financial interests.

Supporting Information

Experimental.

Reaction mechanism.

Kinetic analysis k_1 / k_3 .

Computational methods and (product)reagent-ion cluster stability.

Atmospheric modeling approach.

Figures S1 to S9.

References

- (1) Andreae, M. O. Ocean-atmosphere interaction in the global biochemical sulfur cycle. *Mar. Chem.* **1990**, *30*, 1-29.
- (2) Belviso, S.; Bopp, L.; Moulin, C.; Orr, J. C.; Anderson, T. R.; Aumont, O.; Chu, S.; Elliot, S.; Maltrud, M. E.; Simo, R. Comparison of global climatological maps of sea surface dimethyl sulfide. *Global Biochem. Cy.* **2004**, *18*, GB3013.
- (3) Elliott, S.; Dependence of DMS global sea-air flux distribution on transfer velocity and concentration field type. *J. Geophys. Res.-Biogeo.* **2009**, *114*, 1-18.
- (4) Woodhouse, M. T.; Carslaw, K. S.; Mann, G. W.; Vallina, S. M.; Vogt, M.; Halloran, P. R.; Boucher, O. Low sensitivity of cloud condensation nuclei to changes in the sea-air flux of dimethyl sulfide. *Atmos. Chem. Phys.* **2010**, *10*, 7545-7559.
- (5) Lana, A. *et al.* An updated climatology of surface dimethylsulfide concentrations and emission fluxes in the global ocean. *Global Biochem. Cy.* **2011**, *25*, GB1004.
- (6) Tesdal, J. E.; Christian, J. R.; Monahan, A. H.; von Salzen, K. Evaluation of diverse approaches for estimating sea-surface DMS concentration and air-sea exchange at global scale. *Environ. Chem.* **2016**, *13*, 390-412.
- (7) Barnes, I.; Hjorth, J.; Mihalopoulos, N. Dimethyl sulfide and dimethyl sulfoxide and their oxidation in the atmosphere. *Chem. Rev.* **2006**, *106*, 940-975.
- (8) Charlson, R. J.; Lovelock, J. E.; Angreave, M. O.; Warren, S. G. Oceanic phytoplankton, atmospheric sulphur, cloud albedo and climate. *Nature* **1987**, *326*, 655-661.
- (9) von Glasow, R.; Crutzen, P. J. Model study of multiphase DMS oxidation with a focus on halogens. *Atmos. Chem. Phys.* **2004**, *4*, 589-608.
- (10) Carslaw, K. S. *et al.* Large contribution of natural aerosols to uncertainty in indirect forcing. *Nature* **2013**, *503*, 67-71.
- (11) Hynes, A. J.; Wine, P. H.; Semmes, D. H. Kinetics and mechanism of OH reactions with organic sulfides. *J. Phys. Chem.* **1986**, *90*, 4148-4856.
- (12) Wallington, T. J.; Atkinson, R.; Tuazon, E. C.; Aschmann, S. M. The reaction of OH radicals with dimethyl sulfide. *Int. J. Chem. Kinet.* **1986**, *18*, 837-846.
- (13) Albu, M.; Barnes, I.; Becker, K. H.; Patroescu-Klotz, I.; Mocanu, R.; Benter, Th. Rate coefficient for the gas-phase reaction of OH radicals with dimethyl sulfide: temperature and O₂ partial pressure dependence. *Phys. Chem. Chem. Phys.* **2006**, *8*, 728-736.
- (14) Arsene, C.; Barnes, I.; Becker, K. H. FT-IR product study of the photo-oxidation of dimethyl sulfide: temperature and O₂ partial pressure dependence. *Phys. Chem. Chem. Phys.* **1999**, *1*, 5463-5470.
- (15) Master Chemical Mechanism, MCM v3.3.1, via website: <http://mcm.leeds.ac.uk/MCM>. Last access May 9th, 2019.
- (16) Wallington, T. J.; Ellermann, T.; Nielson, O. J. Atmospheric chemistry of dimethyl sulfide: UV spectra and self-reaction kinetics of CH₃SCH₂ and CH₃SCH₂O₂ radicals and kinetics of the reactions CH₃SCH₂ + O₂ → CH₃SCH₂O₂ and CH₃SCH₂O₂ + NO → CH₃SCH₂O + NO₂. *J. Phys. Chem.* **1993**, *97*, 8442-8449.

- (17) Turnipseed, A. A.; Barone, S. B.; Ravishankara, A. R. Reaction of OH with dimethyl sulfide. 2. Products and mechanism. *J. Phys. Chem.* **1996**, *100*, 14703-14713.
- (18) Urbanski, S. P.; Stickel, R. E.; Zhao, Z.; Wine, P. H. Mechanistic and kinetic study of formaldehyde production in the atmospheric oxidation of dimethyl sulfide. *J. Chem. Soc., Faraday Trans.* **1997**, *93*, 2813-2818.
- (19) Orlando, J. J.; Tyndall, G. S. Laboratory studies of organic peroxy radical chemistry: an overview with emphasis on recent issues of atmospheric significance. *Chem. Soc. Rev.* **2012**, *41*, 6294-6317.
- (20) Wu, R.; Wang, S.; Wang, L. New mechanism for the atmospheric oxidation of dimethyl sulfide. The importance of intramolecular hydrogen shift in a CH₃SCH₂OO radical. *J. Phys. Chem. A* **2015**, *119*, 112-117.
- (21) Moshhammer, K. *et al.* Detection and Identification of the Keto-Hydroperoxide (HOOCH₂OCHO) and Other Intermediates during Low-Temperature Oxidation of Dimethyl Ether. *J. Phys. Chem. A* **2015**, *119*, 7361-7374.
- (22) Berndt, T.; Richters, S. Products of the reaction of OH radicals with dimethyl sulfide in the absence of NO_x: Experiment and simulation. *Atmos. Environ.* **2012**, *47*, 316-322.
- (23) Barnes, I.; Becker, K. H.; Patroescu, I. V. FTIR product study of the OH initiated oxidation of dimethyl sulfide: Observation of carbonyl sulphide and dimethyl sulfoxide. *Atmos. Environ.* **1996**, *30*, 1805-1814.
- (24) Niki, H.; Maker, P. D.; Savage, C. M.; Breitenbach, L. P. An FTIR study of the mechanism for the Reaction HO + CH₃SCH₃. *Int. J. Chem. Kinet.* **1983**, *15*, 647-654.
- (25) Berndt, T.; Kaethner, R.; Voigtländer, J.; Stratmann, F.; Pfeiffle, M.; Reichle, P.; Sipilä, M.; Kulmala, M.; Olzmann, M. Kinetics of the unimolecular reaction of CH₂OO and the bimolecular reactions with the water monomer, acetaldehyde and acetone under atmospheric conditions. *Phys. Chem. Chem. Phys.* **2015**, *17*, 19862-19873.
- (26) Berndt, T. *et al.* Hydroxyl radical induced formation of highly oxidized organic compounds. *Nat. Commun.* **2016**, *7*, 13677.
- (27) Huey, L. G.; Hanson, D. R.; Howard, C. J. Reactions of SF₆⁻ and I⁻ with atmospheric trace gases. *J. Phys. Chem.* **1995**, *99*, 5001-5008.
- (28) Lee, B. H.; Lopez-Hilfiker, F. D.; Mohr, C.; Kurtén, T.; Worsnop, D. R.; Thornton, J. A. An iodide-adduct high-resolution time-of-flight chemical-ionization mass spectrometer: Application to atmospheric inorganic and organic compounds. *Environ. Sci. Technol.* **2014**, *48*, 6309-6317.
- (29) Bertram, T. H.; Kimmel, J. R.; Crisp, T. A.; Ryder, O. S.; Yatavelli, R. L. N.; Thornton, J. A.; Cubison, M. J.; Gonin, M.; Worsnop, D. R. A field-deployable, chemical ionization time-of-flight mass spectrometer. *Atmos. Meas. Tech.* **2011**, *4*, 1471-1479.
- (30) Aljawhary, D.; Lee, A. K. Y.; Abbatt, J. P. D. High-resolution chemical ionization mass spectrometry (ToF-CIMS): application to study SOA composition and processing. *Atmos. Meas. Tech.* **2013**, *6*, 3211-3224.
- (31) Berndt, T.; Scholz, W.; Mentler, B.; Fischer, L.; Herrmann, H.; Kulmala, M.; Hansel, A. Accretion product formation from self- and cross-reactions of RO₂ radicals in the atmosphere. *Angew. Chem. Int. Ed.* **2018**, *57*, 3820-3824.
- (32) Nowak, J. B.; Neuman, J. A.; Kozai, K.; Huey, L. G.; Tanner, D. J.; Holloway, J. S.; Ryerson, T. B.; Frost, G. J.; McKeen, S. A.; Fehsenfeld, F. C. A chemical ionization mass

spectrometry technique for airborne measurements of ammonia. *J. Geophys. Res.* **2007**, *112*, D10S02.

(33) Hansel, A.; Scholz, W.; Mentler, B.; Fischer, L.; Berndt, T. Detection of RO₂ radicals and other products from cyclohexene ozonolysis with NH₄⁺ and acetate chemical ionization mass spectrometry. *Atmos. Environ.* **2018**, *186*, 248-255.

(34) Zaytsev, A.; Breitenlechner, M.; Koss, A. R.; Lim, C. Y.; Rowe, J. C.; Kroll, J. H.; Keutsch, F. N. Using collision-induced dissociation to constrain sensitivity of ammonia chemical ionization mass spectrometry (NH₄⁺-CIMS) to oxygenated volatile organic compounds. *Atmos. Meas. Tech.* **2019**, *12*, 1861-1870.

(35) Kroll, J. H.; Sahay, S. R.; Anderson, J. G.; Demerjian, K. L.; Donahue, N. M. Mechanism of HO_x formation in the gas-phase ozone-alkene reaction. 2. Prompt versus thermal dissociation of carbonyl oxides to form OH. *J. Phys. Chem. A* **2001**, *105*, 4446-4457.

(36) Raff, J. D.; Finlayson-Pitts, B. J. Hydroxyl radical quantum yields from isopropyl nitrite photolysis in air. *Environ. Sci. Technol.* **2010**, *44*, 8150-8155.

(37) Williams, M. B.; Campuzano-Jost, P.; Hynes, A. J.; Pounds, A. J. Experimental and theoretical studies of the reaction of the OH radical with alkyl sulfides: 3. Kinetics and mechanism of the OH initiated oxidation of dimethyl, dipropyl, and dibutyl sulfides: Reactivity trends in the alkyl sulfides and development of a predictive expression for the reaction of OH with DMS. *J. Phys. Chem. A* **2009**, *113*, 6697-6709.

(38) Crounse, J. D.; Paulot, F.; Kjaergaard, H. G.; Wennberg, P. O. Peroxy radical isomerization in the oxidation of isoprene. *Phys. Chem. Chem. Phys.* **2011**, *13*, 13607-136130.

(39) Iyer, S.; He, X.; Hyttinen, N.; Kurtén, T.; Rissanen, M. P. Computational and experimental investigation of the detection of HO₂ radical and the products of its reaction with cyclohexene ozonolysis derived RO₂ radicals by an iodide-based chemical ionization mass spectrometer. *J. Phys. Chem. A* **2017**, *121*, 6778-6789.

(40) Cox, R. A.; Sheppard, D. Reactions of OH radicals with gaseous sulphur compounds. *Nature* **1980**, *284*, 330-331.

(41) Atkinson, R. Kinetics and mechanism of the gas-phase reactions of the hydroxyl radical with organic compounds under atmospheric conditions. *Chem. Rev.* **1985**, *85*, 69-201.

(42) Atkinson, R.; Aschmann, S. M.; Carter, W. P. L. Rate constants for the gas-phase reactions of OH radicals with a series of bi- and tricycloalkanes at 299 ± 2 K: Effects of ring strain. *Int. J. Chem. Kinet.* **1983**, *15*, 37-50.

(43) Wolke, R.; Sehili, A. M.; Simmel, M.; Knoth, O.; Tilgner, A.; Herrmann, H. SPACCIM: A parcel model with detailed microphysics and complex multiphase chemistry. *Atmos. Environ.* **2005**, *39*, 4375-4388.

(44) Hoffmann, E. H.; Tilgner, A.; Schrödner, R.; Bräuer, P.; Wolke, R.; Herrmann, H. An advanced modeling study on the impacts and atmospheric implications of multiphase dimethyl sulfide chemistry. *Proc. Natl. Acad. Sci. USA* **2016**, *113*, 11776-11781.

(45) Daykin, E. P.; Wine, P. H. A study of the reactions of NO₃ radicals with organic sulfides. Reactivity trend at 298 K. *Int. J. Chem. Kinet.* **1990**, *22*, 1083-1094.

